



# Deficiency of ovarian ornithine decarboxylase contributes to aging-related egg aneuploidy in mice

Yong Tao<sup>1,2</sup> and X. Johné Liu<sup>1,2,3,4</sup>

<sup>1</sup>Ottawa Hospital Research Institute, Ottawa Hospital-General Campus, Ottawa, ON, Canada

<sup>2</sup>Faculty of Graduate and Postdoctoral Studies, University of Ottawa, Ottawa, ON, Canada

<sup>3</sup>Department of Obstetrics and Gynaecology, University of Ottawa, Ottawa, ON, Canada

<sup>4</sup>Department of Biochemistry, Microbiology and Immunology, University of Ottawa, Ottawa, ON, Canada

## Summary

It has been known for more than four decades that during mammalian estrous cycles, luteinizing hormone stimulates a transitory rise in the ovaries of ornithine decarboxylase (ODC) activity and its enzymatic product putrescine, concurrent with oocyte maturation *in vivo*. Inhibition of this transitory ODC/putrescine rise, however, does not appear to affect oocyte maturation or ovulation. Using several mouse models and combining *in vitro* and *in vivo* approaches, we demonstrated that deficiency of ODC during oocyte maturation is correlated with increased levels of egg aneuploidies. These results suggest that the transitory ovarian ODC rise in late proestrus is important for ensuring proper chromosome segregation during oocyte maturation. Older mice (8 months of age) exhibited about 1/3 that of young mice in LH-stimulated ovarian ODC activity and a corresponding increase in egg aneuploidies. Moreover, a combination of putrescine supplementation in mouse drinking water leading up to oocyte retrieval and in oocyte maturation medium reduced egg aneuploidies of the older mice from 12.7% to 5.3%. Therefore, ovarian ODC deficiency might be an important etiology of maternal aging-related aneuploidies, and peri-ovulatory putrescine supplementation might reduce the risk of aneuploid conceptions in older women.

**Key words:** aging; aneuploidy; anti-aging; Down Syndrome; meiosis; mice; ornithine decarboxylase; putrescine; reactive oxygen species.

## Introduction

Ornithine decarboxylase (ODC) is an essential enzyme in all eukaryotes, from yeasts (Whitney & Morris, 1978) to mammals (Pendeville *et al.*, 2001), due to its role in cell replication. Consistent with this role, during mouse embryogenesis ODC expression increases sharply after implantation (E6–E8), at a time of rapid cell proliferation (Fozard *et al.*, 1980a). Chemical inhibition (Fozard *et al.*, 1980a) or gene knockout (Pendeville *et al.*, 2001) invariably causes embryonic death at this period. On the

other hand, the function of ODC during mammalian ovulation remains enigmatic (Lefevre *et al.*, 2011). During estrous cycles in rats (Kobayashi *et al.*, 1971) and mice (Bastida *et al.*, 2005), ovarian ODC activity, and the corresponding ovarian putrescine concentration (Fozard *et al.*, 1980b; Bastida *et al.*, 2005) exhibit a LH-mediated transitory rise during the evening of proestrus, concurrent with oocyte maturation *in vivo*. This level of ODC activity is at least 10 times that required for the preceding follicular phase, which is characterized by significant cell proliferation within the antral follicles (Kobayashi *et al.*, 1971; Fozard *et al.*, 1980b; Bastida *et al.*, 2005), suggesting a function(s) unrelated to cell proliferation. Within the ovaries, LH stimulates the transitory rise of ODC proteins mainly in preovulatory follicles (Ickeson *et al.*, 1974), both in the somatic (theca and granulosa) cells and in the oocytes (Bastida *et al.*, 2005). Complete inhibition of this transitory ODC/putrescine rise does not affect oocyte maturation or ovulation (Fozard *et al.*, 1980b; Bastida *et al.*, 2005). It has been suggested that the transitory rise of ovarian ODC activity is required for luteinization of the granulosa cells to produce progesterone (Bastida *et al.*, 2005), although gestation appears normal when the transitory ODC/putrescine rise is inhibited (Fozard *et al.*, 1980b). Similarly, oocyte maturation in *Xenopus laevis*, a species lacking luteinization or implantation, is also accompanied by significant and transitory rise in ODC activity (Younglai *et al.*, 1980; Sunkara *et al.*, 1981; Zhou *et al.*, 2009). We have shown that ODC activity rise during frog oocyte maturation is due to *de novo* protein translation and that its complete inhibition, although not affecting polar body emission, leads to increase in oxidative stress and apoptosis (Zhou *et al.*, 2009).

We have undertaken to study the possible function of ODC in mouse oocyte maturation. Inhibition of ODC activity did not interfere with polar body emission and metaphase II arrest. However, upon karyotyping metaphase II eggs, we discovered that ODC-deficient eggs exhibited a significant increase in aneuploidies. ODC inhibition similarly increased egg aneuploidies in a mouse model exhibiting ‘near-human aneuploidy levels’ (Koehler *et al.*, 2006). The impact of ODC deficiency on egg aneuploidies was also demonstrated *in vivo* by including ODC inhibitor in mouse drinking water for 48 hours leading up to ovulation. Older mice exhibited diminished LH-induced ovarian ODC activity and elevated egg aneuploidy. Most importantly, putrescine supplementation reduced egg aneuploidy rate in these older mice, suggesting ovarian ODC deficiency as an important etiology for maternal age-related aneuploidies.

## Results

LH stimulates ODC expression in preovulatory follicles (Ickeson *et al.*, 1974), both in the oocytes and in somatic (theca and granulosa) cells (Bastida *et al.*, 2005). To determine whether inhibition of oocyte ODC activity affects mouse oocyte *in vitro* maturation (IVM), we employed  $\alpha$ -difluoromethylornithine (DFMO), an enzyme-activated irreversible inhibitor for eukaryotic ODC (Metcalf *et al.*, 1978; Poulin *et al.*, 1992; Pegg, 2006). Immature mouse oocytes (aka ‘GV oocytes’ for the presence of intact germinal vesicle) from young CF1 mice (7–8 weeks of age) were cultured in medium (control) or medium containing 5 mM DFMO (Garcia-Faroldi *et al.*, 2009). DFMO in oocyte IVM medium did not affect spindle assembly (not shown) or first polar body emission (776/

## Correspondence

X. Johné Liu, Ottawa Hospital Research Institute, The Ottawa Hospital - General Campus, 501 Smythe Road, box 511, Ottawa, K1H 6X9, Ontario. Tel: 613 798-5555 extn. 72906; Fax: 613 739-6968; e-mail: jliu@ohri.ca

Accepted for publication 02 October 2012

945 or 82%, compared with 676/843 or 80.2% for control), consistent with our observation in frog oocytes (Zhou *et al.*, 2009).

We subjected all metaphase II eggs to karyotype analyses and counted spreads that contained 18 or more chromosomes and in which all chromosomes were close together (supplementary Fig. S1), to eliminate over-spread karyotypes. Only hyperploid eggs, those containing 21 or more chromosomes, are considered aneuploid, to avoid artifacts due to loss of chromosomes during preparation of chromosome spreads (Koehler *et al.*, 2006). In this set of experiments, in which only DNA staining was employed, we did not distinguish hyperploid oocytes that contained extra whole-chromosomes (dyads) from those that contained separated sister(s), because it is often difficult to differentiate a small chromosome dyad and a single sister in telocentric chromosomes such as in mouse (supplementary Fig. S1). Nonetheless, these results indicated a significant increase in aneuploidies in oocytes treated with DFMO during IVM (Table 1 and supplementary Table S1). To confirm the specificity of DFMO in ODC inhibition, we carried out rescue experiments in which 5 mM putrescine (Zhou *et al.*, 2009) was added together with DFMO to the IVM medium. Our analyses of a relatively small number of oocytes suggested that putrescine supplementation reduced egg aneuploidies caused by DFMO (Table 1).

We next examined the effect of DFMO on egg aneuploidy *in vivo*. We first confirmed that DFMO in mouse drinking water (Nilsson *et al.*, 2005) (1%; see supplementary Fig. S2 for details) efficiently inhibited ovarian ODC activity (Fig. 1A, B, compare 'hCG+DFMO' to 'hCG' in 8-week-old mice). Oviduct-derived metaphase II eggs, from control mice and DFMO-treated mice, were subjected to karyotype analyses. In these and all subsequent egg karyotype analyses, we used anti-CREST antibodies to label centromeres/kinetochores (Hodges & Hunt, 2002), in addition to DNA staining. This modification allowed unambiguous identification of single sister chromatid(s) in metaphase II eggs, termed premature separation of sister chromatids (PSSC, Fig. 2A), the predominant form of mouse egg aneuploidies found in this study (see Table 2). DFMO did not affect the number of MII eggs collected from the oviducts (control: 28.6/mouse,  $n = 38$  vs. DFMO: 29.3/mouse,  $n = 37$ ), indicating normal folliculogenesis and ovulation. However, DFMO caused a significant increase in aneuploidies in ovulated eggs, from 1.3% to 7.7%. Furthermore, a majority of the aneuploidies involved PSSC (Table 3, and Table S2). To rule out any possibility that chromosome spreading procedures may artificially separate sister chromatids and complicate the DFMO results, we carried out 2-cell embryo karyotyping, which does not rely on the presence of single sister chromatids (Fig. 2B). Again, DFMO

**Table 1** DFMO increases aneuploidy rate of young CF1 mice *in vitro*

Treatment	N (cells)	Hypoploid		Euploid	Hyperploid		%Hyperploidy
		18	19	20	21	22	
Control	287	10	23	251	3	0	1.0
DFMO	205	2	18	175	10	0	4.9*
DFMO+Put	95	1	16	76	2	0	2.1**/***

GV oocytes from 7 to 8-week-old CF1 mice were incubated for 17 h in  $\alpha$ MEM (control),  $\alpha$ MEM with 5 mM DFMO, or  $\alpha$ MEM with 5 mM DFMO together with 5 mM putrescine. Metaphase II eggs were karyotyped with chromosome staining only. N, total number of interpretable metaphase II spreads, with 18 or more chromosomes. Hypoploid: 18–19 chromosomes. Euploid: 20 chromosomes. Hyperploid: 21 chromosomes. Detailed breakdowns are available in supplemental Table S1.

\* $P = 0.0186$  compared to control.

\*\* $P = 0.6014$  compared to control; \*\*\* $P = 0.3509$  compared to DFMO.

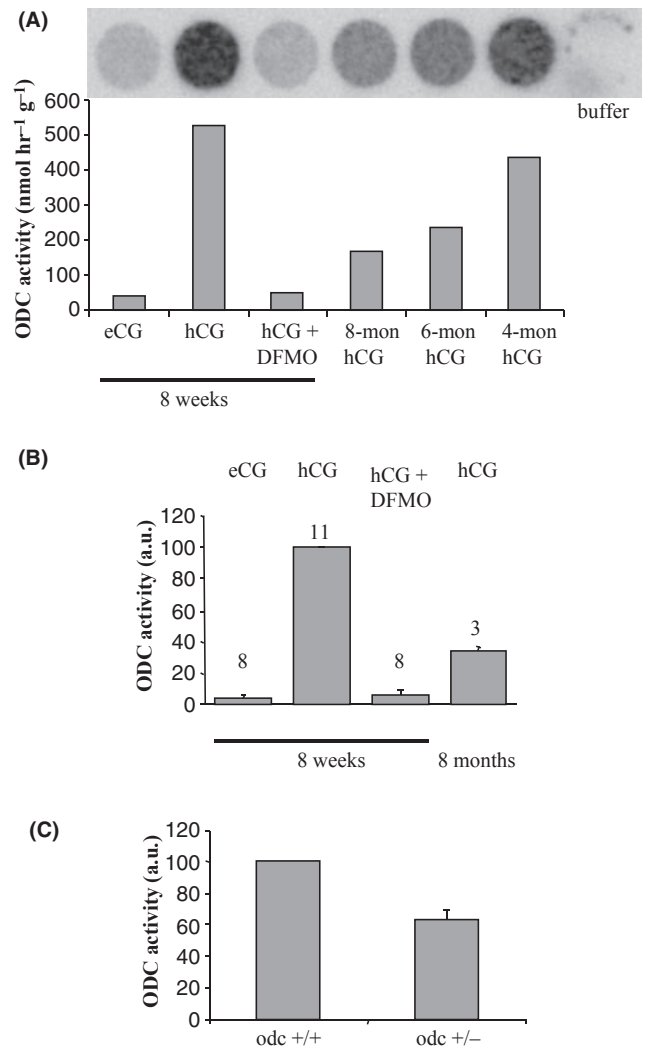


**Fig. 1** Mouse ovary ODC activity assays. (A) A representative (C57BL/6) ovarian ODC activity assay, with 2 mg of ovarian tissues in each sample. Shown on top is the image generated from scanning the Storage phosphor screen that had been exposed to the Ba<sup>14</sup>CO<sub>3</sub> reaction strip. The far right well contained ovarian extraction buffer as negative control. ODC activity is expressed as nmol CO<sub>2</sub> released per hour per gram of ovarian tissues. (B) Ovarian ODC activity, in arbitrary units relative to hCG-stimulated young (8-week-old) C57BL/6 mice (set at 100), of eCG-primed young C57BL/6 mice, hCG-stimulated young C57BL/6 mice, hCG-stimulated young C57BL/6 mice with 48 h DFMO in drinking water, and hCG-stimulated 8-month-old C57BL/6 mice. Shown are means with standard deviations of 3–11 determinations (indicated), each with a different mouse. (C) Ovarian ODC activity of 8-week-old *odc*<sup>+/-</sup> compared with the wild-type littermate. Shown are means (with standard deviations) of three independent experiments, each with wild-type mice set at 100 a.u. (arbitrary units).

treatment significantly increased the occurrence of hyperploid 2-cell embryos, from 0 to 10.4% (Table 4, and Table S3).

Two other mouse models were employed in this study. First, we tested if DFMO treatment could also increase egg aneuploidy in the hybrid F1 females that has a high baseline aneuploidy rate similar to human (Koehler *et al.*, 2006). The interspecies F1 females, from crossing female C57BL/6 (*Mus musculus*) and male SPRET/Ei mice (*Mus spretus*), exhibit impaired non-sister crossovers and therefore predispose oocytes to an increased risk of aneuploidy (Koehler *et al.*, 2006). We showed that MII eggs derived from IVM of young F1 females exhibited a high

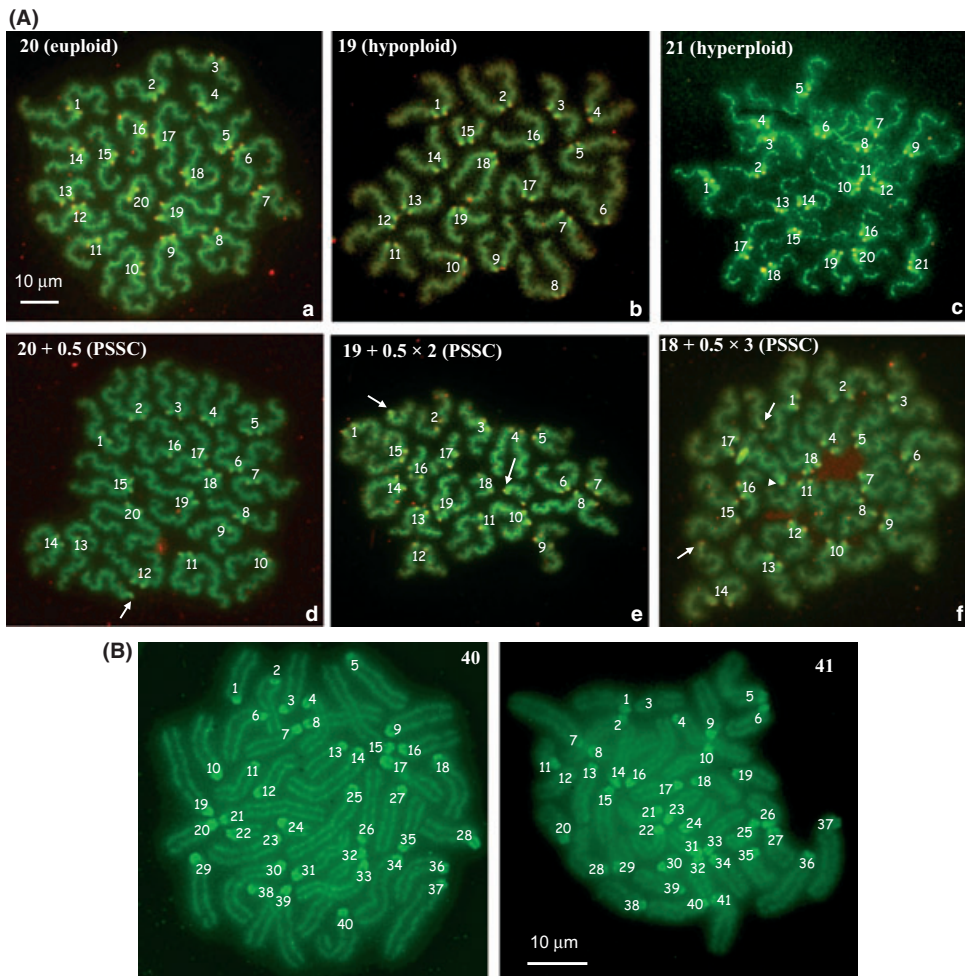


**Fig. 2** Typical karyotype images of metaphase II mouse eggs and 2-cell embryo blastomeres. (A) Representative merged images (green for DNA and red for CREST) of a euploid metaphase II egg (a, 20 dyads), a hypoploid metaphase II egg (b, 19 dyads), a hyperploid metaphase II egg (c, 21 dyads), and three PSSC metaphase II eggs with one (d), two (e), and three (f) separated sister chromatids (arrows or arrow head), respectively. The two sister chromatids in e appear to belong to the same chromosome. Similarly in f, two of the three separated sisters (arrows) appear to belong to the same chromosome. Numbers 1–21 are used to facilitate chromosome counting and do not imply chromosome identities. (B) Representative 2-cell embryo blastomere karyotypes showing 40 chromosomes (euploid) or 41 chromosomes (hyperploid). Numbers 1–41 are used to facilitate chromosome counting and do not imply chromosome identities.

aneuploidy rate (12.1%) comparable to that (10.1%) previously determined in ovulated eggs (Koehler *et al.*, 2006). The presence of 5 mM DFMO in IVM medium indeed significantly increased egg aneuploidy rate to 22.5% (Table 5, and Table S4). Second, we examined if heterozygous *odc* mice (Pendevelle *et al.*, 2001) exhibit elevated egg aneuploidy. Analyzing ovarian ODC activity indicated ~40% reduction in heterozygous *odc* mice, compared with age-matched wild-type littermates (Fig. 1C). Analyzing oviduct-derived eggs indicated an elevation in egg aneuploidy in heterozygous *odc* mice, compared with age-matched wild-type littermates, although the difference has not reached statistical significance (Table 6, and Table S5).

Do older mice exhibit ovarian ODC deficiency and, if so, does it contribute to the increased egg aneuploidy observed in their oocytes? We found aging-dependent reduction of ovarian ODC activity, reaching ~1/3 in 8-month-old C57BL/6 mice (Fig. 1A, B). We chose 8-month-old mice for this work because these mice satisfy two competing conditions for our study: these mice exhibit diminished ovarian ODC activity (above), and these mice produce as many eggs as young mice (Harman & Talbert, 1970), the latter of which is important for generating good quality aneuploidy data. In addition, the fact that these mice were healthy (reproductively and otherwise) and yet had diminished ovarian ODC activity means that they serve as excellent subjects to investigate the importance of ovarian ODC deficiency in egg aneuploidy. To determine whether indeed older mice exhibit diminished ODC expression in the oocytes, we carried out immunohistological analyses of ovarian

sections according to Bastida *et al.*, (2005). Using three different animals in each group, we demonstrated that antral follicles in 8-month-old mice exhibited significantly reduced levels of hCG-induced ODC expression in both the oocyte and somatic cells (Fig. 3). To determine whether the diminished ovarian ODC activity contributes to egg aneuploidies in older mice, we carried out rescue experiments using putrescine supplementation. Preliminary experiments with a few mice indicated that injecting 8-month-old C57BL/6 mice with eCG followed by hCG failed to produce consistent ovulation. We therefore carried out IVM experiments, which revealed that oocytes from these mice exhibited high aneuploidy rate (12.7%). For the rescue experiments, we added 1% putrescine to all drinking water for 7 days, refreshed daily, followed by IVM in the presence of 5 mM putrescine. This combination reduced egg aneuploidies to 5.3%. Putrescine supplementation in mouse drinking water did not change the number of fully grown GV oocytes in the ovaries (control: 26.4/mouse,  $n = 12$  vs. 25.3/mouse,  $n = 13$ ; these numbers are similar to the 27.5 produced by 8-week-old C57BL/6 mice, see Fig. S3). Our analyses of 16-month-old *odc*<sup>-/+</sup> mice, with or without putrescine supplementation, revealed no evidence of spindle abnormality or premature polar body emission (Fig. S3).

## Discussion

It has been known for more than four decades that mammalian ovaries exhibit a LH-mediated transitory rise of ODC activity concurrent with

**Table 2** Summary of all karyotypes shown in Tables 3, 5, 6, and 7

N = 1432					
Phenotype	Frequency	Phenotype	Frequency	Phenotype	Frequency
Euploid (72.7%)		PSSC (5.7%)			
20	1041	20 + 0.5 × 2	2	18 + 0.5 × 2	5
Hyperploid (0.70%)		20 + 0.5 × 1	19	18 + 0.5 × 1	5
22	1	19 + 0.5 × 3	1	17 + 0.5 × 5	1
21	9	19 + 0.5 × 2	15	17 + 0.5 × 4	1
Hypoploid (20.9%)		19 + 0.5 × 1	20	17 + 0.5 × 3	1
19	220	18 + 0.5 × 4	2	17 + 0.5 × 2	6
18	80	18 + 0.5 × 3	2	16 + 0.5 × 6	1

PSSC (5.7%) is much more prevalent than whole chromosome nondisjunction, estimated by hyperploidy (0.7%), in mouse oocytes.

**Table 3** DFMO increases aneuploidy rate of young CF1 mice *in vivo*

Treatment	N (cells)	Hypoploid		Euploid	Hyperploid		PSSC	%Hyperploidy	%Aneuploid
		18	19	20	21	22			
Control	311	11	39	258	1	0	2	0.3	1.3
DFMO	261	12	41	191	3	0	14*	1.1**	7.7***

Young (7–8 weeks) CF1 mice were treated with regular drinking water (control) or 1% DFMO drinking water for 48 h (see Fig. S2). Karyotype analyses were carried out by dual stains (anti-CREST and Sytox green) of metaphase II chromosomes (Fig. 2A). N: number of interpretable metaphase II karyotypes containing at least 18 dyads or the equivalent (e.g., 17 dyads plus two separated sister chromatids). Hypoploid: 18–19 dyads. Euploid: 20 dyads. Hyperploid: 21. PSSC: any karyotypes containing separated sister chromatid(s), with the total of at least 18 dyads or the equivalents. Aneuploid: 2 × hyperploid + PSSC. Detailed breakdowns are in supplemental Table S2.

\**P* = 0.0006.

\*\**P* = 0.3358.

\*\*\**P* = 0.0002.

oocyte maturation *in vivo* (Kobayashi *et al.*, 1971), and yet, it remains unknown if this rise has any role in oocyte maturation or ovulation (Fozard *et al.*, 1980b; Bastida *et al.*, 2005). We have provided evidence that this transitory ODC activity rise is required to ensure proper chromosome segregation during oocyte maturation. Therefore, inhibition of the transitory ovarian ODC activity rise (Fig. 1A and B) significantly increased aneuploidies in ovulated eggs (Table 3) and in 2-cell embryos (Table 4). This conclusion is also supported by karyotyp-

**Table 4** DFMO in mouse drinking water increases hyperploid 2-cell embryos

Treatment	N (2-cell)	Euploid 40	Hypoploid 39	Hyperploid 41
Control	59	51 86.4%	8 13.6%	0 0%
DFMO	48	38 79.2%	5 10.4%	5 10.4%*

Young (7–8 weeks) CF1 mice were treated with regular water (control), or 1% DFMO drinking water for 48 h, prior to mating (see Fig. S2 for details). Embryos (2-cell) were isolated and subjected to karyotype analyses. N: Total interpretable 2-cell embryos. Euploid: 40 chromosomes in each of the two blastomeres, or 40 chromosomes in one blastomere with the other blastomere having less than 40 chromosomes or uninterpretable/lost. Hypoploid: 39 chromosomes in each of the two blastomeres, or 39 in one blastomere with the other less than 39 or uninterpretable/lost. Hyperploid: 41 chromosomes in at least one blastomere (we found no 42 or more chromosomes in this study). Detailed breakdowns are in Table S3.

\**P* = 0.0161.

ing ovulated eggs in heterozygous *odc*<sup>-/+</sup> mice. In this case, a more modest increase in aneuploidies (Table 6) was correlated with a 40% reduction in ovarian ODC activity (Fig. 1C), compared with the significant aneuploidy increase (Tables 3 and 4) in DFMO-treated mice with greater than 90% inhibition of ODC activity (Fig. 1A, B). The very similar low levels of aneuploidies in control eggs regardless of whether denuded oocytes were matured *in vitro* (Table 1) or follicle-enclosed oocytes were matured *in vivo* (Table 3), together with the ability of DFMO to increase egg aneuploidies in IVM experiments (Table 1 and Table 5, for regular mice and the interspecies crossing F1 mice respectively), suggest that ODC activity within the oocytes fulfills this role. On the other hand, the transitory ODC rise within the somatic cells of preovulatory follicles, which represent bulk of the ovarian ODC rise (Ickson *et al.*, 1974), may have multiple functions, including luteinization of the granulosa cells (Bastida *et al.*, 2005) and supporting healthy oocyte maturation *in vivo*. Further investigation is warranted to unravel the physiological roles and molecular mechanisms of this important metabolic pathway in mammalian reproduction.

It remains unknown how ODC/putrescine deficiency increases aneuploidies. We found no evidence of spindle abnormality, either in ODC-deficient young oocytes (not shown) or in oocytes of 16-month-old heterozygous *odc* mice (Fig. S3). The prevalence of PSSC in ODC-deficient young eggs (Tables 3 and 5) suggests that optimal putrescine concentration may have an important role in maintaining sister chromatid cohesion during meiosis I. This role is likely indirect (e.g., via its suppression of oxidative stress, as we have demonstrated during frog oocyte maturation (Zhou *et al.*, 2009)), given the low phenotypic penetrance, in both the number of aneuploid oocytes and the number of

**Table 5** DFMO increases the egg aneuploidy rate of young hybrid F1 females

Treatment	N (cells)	Hypoploid		Euploid	Hyperploid		PSSC	%Hyperploidy	%Aneuploidy
		18	19	20	21	22			
Control	248	13	33	175	2	1	24	1.2	12.1
DFMO	80	5	9	50	2	0	14*	2.5**	22.5***

GV oocytes isolated from young (7–8 weeks) hybrid F1 females, via crossing C57BL/6 females and SPRET/Ei males, were incubated for 17 h in  $\alpha$ MEM (control) or  $\alpha$ MEM containing 5 mM DFMO. Karyotype analyses and data expression were as described in the legend to Table 3.

\* $P = 0.0702$ .

\*\* $P = 0.5989$ .

\*\*\* $P = 0.0287$ .

**Table 6** Heterozygous *odc* mice exhibits a slight increase in egg aneuploidy rate *in vivo*

Genotype	N (cells)	Hypoploid		Euploid	Hyperploid		PSSC	%Hyperploidy	%Aneuploidy
		18	19	20	21	22			
<i>odc</i> +/+	149	15	42	91	0	0	1	0	0.7
<i>odc</i> +/-	127	13	23	87	0	0	4	0	3.1*

Young (7–8 weeks) *odc* +/- and *odc* +/+ mice were superovulated. Oviduct-derived metaphase II eggs were karyotyped and data expressed as described in Table 3.

\* $P = 0.1839$ .

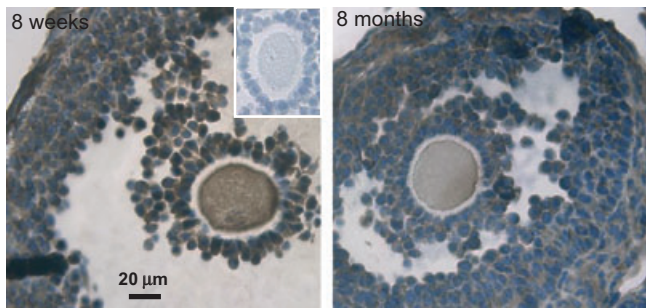


**Fig. 3** ODC expression in pre-ovulatory follicles of young and older mice. Young (8 weeks) and older (8 months) C57BL/6 mice were injected with eCG and, 44–46 hours later, with hCG. Six hours following hCG injection, ovaries were excised and processed for immunohistochemical analyses using anti-ODC antibodies. Shown are representative images (three animals in each group, three staining experiments) of pre-ovulatory follicles from young (left) and older (right) mice. Inset is a negative control in which no primary antibodies were added.

chromosomes in affected oocytes, even when the transitory ODC rise was virtually eliminated (Fig. 1A, B). PSSC is also the dominant form of aneuploidies in eggs of older mice (Table 7), which exhibited significantly reduced level of ODC (Fig. 3). Therefore, aging-related partial loss of chromosome-associated cohesin predisposes these oocytes to increased risk of losing centromeric cohesion in meiosis I (Chiang *et al.*, 2010; Lister *et al.*, 2010; Duncan *et al.*, 2012). This increased risk, together with the diminished ODC activity (Fig. 1A, B, and Fig. 3), leads to increased incidence of PSSC. Restoration of optimal putrescine concentrations in the ovaries and the oocytes of older mice appeared to protect at least some of the vulnerable centromeric cohesion during meiosis I (Table 7).

Our finding of PSSC as the dominant form of aneuploidies in ODC-deficient mice (8-week-old and 8-month-old, see Table 2 for summary) is in contrast to the recent studies that suggest whole-chromosome nondisjunction as the main form of aneuploidies in aged mice (Selesniemi *et al.*, 2011; Merriman *et al.*, 2012). While Selesniemi

**Table 7** Putrescine supplementation reduces egg aneuploidy in older mice

Treatment	N (cells)	Hypoploid		Euploid	Hyperploid		PSSC	%Hyperploidy	%Aneuploidy
		18	19	20	21	22			
Control	142	7	12	106	1	0	16	0.7	12.7
Putrescine	114	4	21	83	0	0	6	0	5.3*

C57BL/6 (8 months) mice were treated with regular drinking water (control) or 1% putrescine drinking water for 1 week. GV oocytes isolated from the ovaries of control mice were incubated for 17 h in  $\alpha$ MEM. Oocytes isolated from putrescine treated mice were incubated for 17 h in  $\alpha$ MEM containing 5 mM putrescine. Metaphase II eggs following IVM were karyotyped and data expressed as described in Table 3.

\* $P = 0.0523$ .

*et al.* (2011) employed DAPI staining of chromosomes in karyotyping, Merriman *et al.* (2012) employed a novel *in situ* karyotyping method based on fluorescence confocal imaging of monastral-treated oocytes (Duncan *et al.*, 2009). This method, which stains both chromosomes and centromeres/kinetochores (CREST) in fixed oocytes, has the distinct advantage of preserving all chromosomes (Duncan *et al.*, 2009; Merriman *et al.*, 2012). However, its identification of PSSC based on odd number of CREST dots (Merriman *et al.*, 2012) likely underestimates the incidence of PSSC, as karyotypes that contain two separated sister chromatids are common forms (Fig. 2A, panel e, and Table 2).

In our study, we employed the method developed by Hodges and Hunt (Hodges & Hunt, 2002) that involves the prior removal of zona pellucida so that the eggs are gently lysed in a hypotonic buffer [instead of the methanol/acidic acid fixative in the classical Takowski protocol (Evans, 1987)] during chromosome spreading. As a result, chromosomes remain closely and evenly positioned, often in a circular array, suggesting that all chromosomes 'touch down' on the glass slide while still being associated with the spindle. This method also has the distinct advantage of preserving chromosome-associated proteins including CREST antigens (Hodges & Hunt, 2002), allowing simultaneous visualization of chromosomes and centromeres and hence unambiguous identification of PSSC. In all PSSC spreads, very few, mostly just one or two, separated sisters were present together with perfectly preserved chromosome dyads (Fig. 2A and Table 2), arguing against any possibility that the sisters are separated as a result of procedural artifact. Furthermore, in those PSSC karyotypes with two (or more) separated sisters, the sisters were randomly positioned among, and neatly fitted into, the chromosome array with no association with one another (Fig. 2A, panels e and f), consistent with being single sisters in the metaphase II spindle before spreading. Interestingly, in most, if not all, of the oocytes (Table 2) involving two separated sisters (Fig. 2Ae), the sisters appeared to belong to the same chromosome. Therefore, the affected sisters were segregated correctly during oocyte maturation (anaphase I) but became separated before the assembly of the metaphase II spindle in the mature egg. Such segregation errors appear to be the major form of aneuploidies in older oocytes, as supported by live cell imaging studies (Chiang *et al.*, 2010). Finally, we have employed an independent method, karyotyping 2-cell embryos, which does not rely on separated sisters, to confirm the key finding that ODC deficiency causes increased aneuploidies (Fig. 2B and Table 4). The absence of hyperploid 2-cell embryos (0/59) in the control group indicates the extremely low incidence of aneuploidies in sperm and in first embryo mitosis, thus validating this as an alternative method of karyotyping the eggs.

Earlier studies by Angell and colleagues of surplus human IVF eggs have concluded that PSSC is the dominant form of aneuploidies and whole-chromosome nondisjunction is rare (Angell, 1991, 1997; Angell *et al.*, 1994). Others have reported both PSSC and whole-chromosome nondisjunction in human eggs (Dailey *et al.*, 1996; Mahmood *et al.*, 2000). In contrast to these earlier studies, which involved relatively small number of human eggs, Kuliev *et al.* (2011) analyzed more than 20,000 human eggs (via their polar bodies) and concluded that, among the overall 31.1% aneuploidies, 93.7% are of PSSC phenotypes and only 6.3% are whole-chromosome nondisjunction. This large study provides compelling support for the Angell hypothesis that PSSC is the dominant form of human egg aneuploidies (Wolstenholme & Angell, 2000); it also reiterates the extraordinarily high incidence of human egg aneuploidies, 31.1% with only five of the 23 chromosomes analyzed (Kuliev *et al.*, 2011).

It is estimated that only 30% of human conceptions result in live births. Another 10% are spontaneously aborted. The majority, 60%, are thought to be lost prior to clinical recognition of pregnancy (Baird *et al.*, 2005). Egg aneuploidy, with dramatically increased incidences in older women, likely plays a dominant role in these 'missing' human embryos, in miscarriages, and in birth defects (Hassold & Hunt, 2001). If a causal relationship exists in humans between ovarian ODC deficiency and egg aneuploidies, peri-ovulatory putrescine supplementation may be an effective intervention in the reproductive health of older women.

## Experimental procedures

### Animals

Animal protocols have been approved by the Animal Care Committee of the Ottawa Hospital Research Institute. CF1 mice and C57BL/6 mice were from Charles River (St-Constant, PQ, Canada). SPRET/Ei mice (*Mus spretus*) were from Jackson lab (Bar Harbor, Maine, US). F1 hybrids were generated by crossing C57BL/6 females to SPRET/Ei males. Heterozygous *odc* mice were produced in house and genotyping carried out according to Penderville *et al.* (2001). The animals were provided with water (or with the indicated drugs) and mouse chow *ad libitum* and housed in rooms illuminated for 12 h/day.

### Oocyte isolation and *in vitro* culture

Mice were euthanized by cervical dislocation 44–46 h after they were primed with 5 IU equine chorionic gonadotropin (eCG) intraperitoneally. For putrescine supplementation, 1% putrescine was in all drinking water for 7 days until euthanization. Ovaries were immediately removed and minced in M2 medium (Sigma; unless otherwise indicated, other chemicals used in this study were also purchased from Sigma) to release oocytes. Oocytes with a clear germinal vesicle (GV) were used for IVM for 17 hours in IVM medium ( $\alpha$ MEM medium supplemented with 5% fetal bovine serum and 1 mM L-glutamine) overlaid with mineral oil.

To collect mature (metaphase II) oocytes *in vivo* (ovulation experiments) each mouse was injected with 5 IU human chorionic gonadotropin (hCG) intraperitoneally 44–46 h after eCG priming. The animals were euthanized 16–18 h after hCG injection and MII eggs were flushed out of oviducts in M2 medium and subjected to karyotype analyses as described below. For mice that were treated with 1% DFMO in drinking water, the drugs were present until the time of euthanization (see Fig. S2).

To produce 2-cell embryos, mice were sequentially injected with eCG and hCG, as above for ovulation. After hCG injection, the females were caged singly with fertile young males overnight. For mice that were treated with 1% DFMO, the drug was withdrawn, and normal water resumed at the time of hCG injection (see Fig. S2). The females were separated from the males in the next morning (day 1 post coital or p.c.). Females were euthanized in the late morning on day 2 p.c., and the embryos were collected by flushing the oviducts with M2 medium. After three rinses in KSOM medium, the embryos were cultured 17 h in KSOM containing 0.02  $\mu$ g/mL colchicine to cause metaphase arrest of the 2-cell embryos.

### Oocyte and embryo chromosome spread

Chromosome spread was carried out according to Hodges and Hunt (Hodges & Hunt, 2002) with minor modifications. In brief, oocytes or 2-

cell embryos were collected in M2 medium. The zona pellucida was removed by treatment with 0.5 units/ $\mu\text{L}$  pronase at 37 °C for 20 sec. Zona-free oocytes/embryos were rinsed in M2 medium to detach polar bodies. The oocytes/embryos were individually plated onto glass slides (1–10 oocytes/embryos per slide) pre-dipped in the fixative (prepared weekly and stored at 4 °C) containing 1% paraformaldehyde (w/v), 0.15% Triton X-100 (v/v), and 3 mM dithiothreitol, pH 9.2. Slides were kept overnight in moist boxes at room temperature. The slides were then rinsed in 0.5% Kodak Photo-Flo200 (Eastman Kodak Company, Rochester, NY, USA) solution and air-dried. The slides were incubated in 1:200 diluted human anti-centromere serum (i.e. CREST serum; Immunovision, Springdale, AR) in PBS containing 1% BSA overnight at 4 °C, in 1:300 diluted secondary antibody (goat anti-human) conjugated with rhodamine (Jackson ImmunoResearch) in PBS-BSA for 1 h at room temperature, and 0.1% SYTOX green (Invitrogen, Eugene, Oregon) in PBS for 30 min at room temperature. To avoid bias, the slides were coded by a colleague before being examined by YT using epifluorescence microscopy and photographed. Decoding was carried out after karyotypes were tabulated.

### ODC activity assay

After 44–46 h eCG priming, or 6 h following the subsequent hCG injection, the ovaries were collected into Eppendorf tubes and frozen at –80 °C immediately till use. The ovaries were weighed and minced with optical scissors. Lysis buffer [25 mM Tris/HCl pH 7.2, 2 mM dithiothreitol, 0.1 mM EDTA, 0.25 M sucrose, 0.1 % Triton X-100 (w/v); modified from Bastida *et al.* (2005)] was added 25  $\mu\text{L}$  per mg ovarian tissues and the resulting suspension homogenized by sonication (Fisher Sonic Dismembrator, New York, USA) for 20 seconds thrice. The ovarian homogenates were centrifuged at 16,000  $\times g$  for 10 min. Supernatants were applied to ODC assays (Zhou *et al.*, 2009) in microtiter plates, each well containing 50  $\mu\text{L}$  of lysate, plus 0.1 mM pyridoxyl-5-phosphate, and 0.5  $\mu\text{Ci}$  (57.1 mCi/mmol) of  $^{14}\text{C}$ -labeled ornithine (PerkinElmer, Boston, MA). The wells were tightly covered with 3 MM paper pre-wet in freshly prepared water-saturated  $\text{Ba}(\text{OH})_2$ . The wells were incubated 1 h at 37°C.  $^{14}\text{CO}_2$  released from decarboxylation reaction formed  $\text{Ba}^{14}\text{CO}_3$  precipitates on filter. The 3 MM paper was exposed to a Storage phosphor screen overnight to capture the latent images produced by  $^{14}\text{C}$ -emitted  $\beta$  radiation. The Storage phosphor screen was then scanned on TYPHOON™ imaging system (GE Healthcare Life Sciences, Amersham, UK), resulting in digital images that were then quantified by Image QUANT 5.2 (GE Healthcare Life Sciences). ODC activity is expressed as relative light intensity in arbitrary units. To determine the absolute ODC activity in ovarian extracts (Fig. 1A), the reaction strips with captured  $\text{Ba}^{14}\text{CO}_3$  were exposed to the Storage phosphor screen alongside a strip spotted with a dilution series of known quantities of  $^{14}\text{C}$ -labeled ornithine, used for calibration.

### Immunohistochemistry

Ovaries were removed 6 hours after hCG injection and fixed in 10% formalin in PBS (pH 7.4) for 10 h. After rinsing in PBS, the samples were dehydrated in a graded ethanol series and embedded in paraffin and then cut in 5  $\mu\text{m}$  sections. The ovarian sections were deparaffinized in xylene and hydrated. Antigen retrieval was undertaken in boiling sodium citrate solution (10 mM, pH 6.0) containing 0.05% Tween 20 for 20 min. After rinsing in TBST (50 mM Tris, pH 7.6, 150 mM NaCl, 0.025% Triton X-100), the sections were blocked in 10% fetal bovine serum with 1% BSA in TBS (50 mM Tris, pH 7.6, 150 mM NaCl) for 2 h at

room temperature and incubated in 1:200 diluted polyclonal antibodies to ODC (rabbit anti-mouse ODC from Acris, Germany) in TBS with 1% BSA at 4 °C overnight. After washing in TBST, the slides were incubated in 0.3% peroxide hydrogen in TBS for 15 min to destroy endogenous peroxidase activity. Sections were then incubated in 1:200 horseradish peroxidase-conjugated secondary antibodies (Biorad, Philadelphia, USA) in TBS with 1% BSA for 2 h at room temperature. The peroxidase activity was visualized with DAB Chromogen (Dako, Carpinteria, USA; diluted to 0.6% in Substrate Buffer) for 2 min. Finally, the sections were counterstained with hematoxylin, dehydrated, cleared, and mounted in Organo/Limonene Mounting medium (Santa Cruz, CA, USA). In the control, anti-ODC antibody was substituted by TBS. Image acquisition was performed on a Zeiss Axiovert 100 (20  $\times$  objective) equipped with a Retiga 1300 CCD camera, using QCAPTURE (version 1.91). White balance was set using a clean and blank slide and all images were taken with identical settings.

### Statistics

All statistical analyses were performed using GRAPHPAD PRISM 5.02. The data in chromosomal spread were analyzed by Fisher's exact test (two-tailed). The *P*-values are indicated in the tables.

### Acknowledgements

We thank Ruizhen Li for technical support, Dr. Patrick Woster (Wayne State University) for the gift of DFMO, Dr. John Cleveland (the Scripps Research Institute) for *odc*<sup>-/-</sup> mice, Drs. Patricia Hunt and Terry Hassold (Washington State University) for advice on oocyte karyotyping and on crossing C57BL/6 females with SPRET/Ei males, and Dr. Jay Baltz (Ottawa Hospital Research Institute) for discussion and comments on the manuscript. This work was supported by grants (to XJL) from NSERC (Discovery) and CIHR (MOP-89973), and a partial scholarship from Reproduction, Early Development and the Impact of Health (REDIH) program of the CIHR (to YT).

### References

- Angell RR (1991) Predisposition in human oocytes at meiosis I: a mechanism for trisomy formation in man. *Hum. Genet.* **86**, 383–387.
- Angell R (1997) First-meiotic-division nondisjunction in human oocytes. *Am. J. Hum. Genet.* **61**, 23–32.
- Angell RR, Xian J, Keith J, Ledger W, Baird DT (1994) First meiotic division abnormalities in human oocytes: mechanism of trisomy formation. *Cytogenet. Cell Genet.* **65**, 194–202.
- Baird DT, Collins J, Egozcue J, Evers LH, Gianaroli L, Leridon H, Sunde A, Templeton A, Van SA, Cohen J, Crosignani PG, Devroey P, Diedrich K, Fauser BC, Fraser L, Glasier A, Liebaers I, Mautone G, Penney G, Tarlatzis B (2005) Fertility and ageing. *Hum. Reprod. Update* **11**, 261–276.
- Bastida CM, Cremades A, Castells MT, Lopez-Contreras AJ, Lopez-Garcia C, Tejada F, Penafiel R (2005) Influence of ovarian ornithine decarboxylase in folliculogenesis and luteinization. *Endocrinology* **146**, 666–674.
- Chiang T, Duncan FE, Schindler K, Schultz RM, Lampson MA (2010) Evidence that weakened centromere cohesion is a leading cause of age-related aneuploidy in oocytes. *Curr. Biol.* **20**, 1522–1528.
- Dailey T, Dale B, Cohen J, Munne S (1996) Association between nondisjunction and maternal age in meiosis-II human oocytes. *Am. J. Hum. Genet.* **59**, 176–184.
- Duncan FE, Chiang T, Schultz RM, Lampson MA (2009) Evidence that a defective spindle assembly checkpoint is not the primary cause of maternal age-associated aneuploidy in mouse eggs. *Biol. Reprod.* **81**, 768–776.
- Duncan FE, Hornick JE, Lampson MA, Schultz RM, Shea LD, Woodruff TK (2012) Chromosome cohesion decreases in human eggs with advanced maternal age. *Aging Cell* **11**, 1121–1124.

- Evans EP (1987). Karyotyping and sexing of gametes, embryos and fetuses and in situ hybridization to chromosomes. In *Mammalian Development: A Practical Approach* (Monk M, ed.). Washington DC: IRL Press, pp. 263.
- Fozard JR, Part ML, Prakash NJ, Grove J, Schechter PJ, Sjoerdsma A, Koch-Weser J (1980a) L-Ornithine decarboxylase: an essential role in early mammalian embryogenesis. *Science* **208**, 505–508.
- Fozard JR, Prakash NJ, Grove J (1980b) Ovarian function in the rat following irreversible inhibition of L-ornithine decarboxylase. *Life Sci.* **27**, 2277–2283.
- Garcia-Faroldi G, Correa-Fiz F, Abrighach H, Berdasco M, Fraga MF, Esteller M, Urdiales JL, Sanchez-Jimenez F, Fajardo I (2009) Polyamines affect histamine synthesis during early stages of IL-3-induced bone marrow cell differentiation. *J. Cell. Biochem.* **108**, 261–271.
- Harman SM, Talbert GB (1970) The effect of maternal age on ovulation, corpora lutea of pregnancy, and implantation failure in mice. *J. Reprod. Fertil.* **23**, 33–39.
- Hassold T, Hunt P (2001) To err (meiotically) is human: the genesis of human aneuploidy. *Nat. Rev. Genet.* **2**, 280–291.
- Hodges CA, Hunt PA (2002) Simultaneous analysis of chromosomes and chromosome-associated proteins in mammalian oocytes and embryos. *Chromosoma* **111**, 165–169.
- Icekson I, Kaye AM, Lieberman ME, Lamprecht SA, Lahav M, Lindner HR (1974) Stimulation by luteinizing hormone of ornithine decarboxylase in rat ovary: preferential response by follicular tissue. *J. Endocrinol.* **63**, 417–418.
- Kobayashi Y, Kupelian J, Maudsley DV (1971) Ornithine decarboxylase stimulation in rat ovary by luteinizing hormone. *Science* **172**, 379–380.
- Koehler KE, Schrupp SE, Cherry JP, Hassold TJ, Hunt PA (2006) Near-human aneuploidy levels in female mice with homeologous chromosomes. *Curr. Biol.* **16**, R579–R580.
- Kuliev A, Zlatopolsky Z, Kirillova I, Spivakova J, Cieslak JJ (2011) Meiosis errors in over 20,000 oocytes studied in the practice of preimplantation aneuploidy testing. *Reprod. Biomed. Online* **22**, 2–8.
- Lefevre PL, Palin MF, Murphy BD (2011) Polyamines on the reproductive landscape. *Endocr. Rev.* **32**, 694–712.
- Lister LM, Kouznetsova A, Hyslop LA, Kalleas D, Pace SL, Barel JC, Nathan A, Floros V, Adelfalk C, Watanabe Y, Jessberger R, Kirkwood TB, Hoog C, Herbert M (2010) Age-related meiotic segregation errors in Mammalian oocytes are preceded by depletion of cohesin and Sgo2. *Curr. Biol.* **20**, 1511–1521.
- Mahmood R, Brierley CH, Faed MJ, Mills JA, Delhanty JD (2000) Mechanisms of maternal aneuploidy: FISH analysis of oocytes and polar bodies in patients undergoing assisted conception. *Hum. Genet.* **106**, 620–626.
- Merriman JA, Jennings PC, McLaughlin EA, Jones KT (2012) Effect of aging on superovulation efficiency, aneuploidy rates, and sister chromatid cohesion in mice aged up to 15 months. *Biol. Reprod.* **86**, 49.
- Metcalfe BW, Bey P, Danzin C, Jung MJ, Casara P, Vevert JP (1978) Catalytic irreversible inhibition of mammalian ornithine decarboxylase (E.C.4.1.1.17) by substrate and product analogues. *J. Am. Chem. Soc.* **100**, 2551–2553.
- Nilsson JA, Keller UB, Baudino TA, Yang C, Norton S, Old JA, Nilsson LM, Neale G, Kramer DL, Porter CW, Cleveland JL (2005) Targeting ornithine decarboxylase in Myc-induced lymphomagenesis prevents tumor formation. *Cancer Cell* **7**, 433–444.
- Pegg AE (2006) Regulation of ornithine decarboxylase. *J. Biol. Chem.* **281**, 14529–14532.
- Pendeveille H, Carpino N, Marine JC, Takahashi Y, Muller M, Martial JA, Cleveland JL (2001) The ornithine decarboxylase gene is essential for cell survival during early murine development. *Mol. Cell. Biol.* **21**, 6549–6558.
- Poulin R, Lu L, Ackermann B, Bey P, Pegg AE (1992) Mechanism of the irreversible inactivation of mouse ornithine decarboxylase by alpha-difluoromethylornithine. Characterization of sequences at the inhibitor and coenzyme binding sites. *J. Biol. Chem.* **267**, 150–158.
- Selesniemi K, Lee HJ, Muhlhauser A, Tilly JL (2011) From the cover: prevention of maternal aging-associated oocyte aneuploidy and meiotic spindle defects in mice by dietary and genetic strategies. *Proc. Natl. Acad. Sci. U.S.A.* **108**, 12319–12324.
- Sunkara PS, Wright DA, Nishioka K (1981) An essential role for putrescine biosynthesis during meiotic maturation of amphibian oocytes. *Dev. Biol.* **87**, 351–355.
- Whitney PA, Morris DR (1978) Polyamine auxotrophs of *Saccharomyces cerevisiae*. *J. Bacteriol.* **134**, 214–220.
- Wolstenholme J, Angell RR (2000) Maternal age and trisomy—a unifying mechanism of formation. *Chromosoma* **109**, 435–438.
- Younglai EV, Godeau F, Mester J, Baulieu EE (1980) Increased ornithine decarboxylase activity during meiotic maturation in *Xenopus laevis* oocytes. *Biochem. Biophys. Res. Commun.* **96**, 1274–1281.
- Zhou Y, Ma C, Karmouch J, Katbi HA, Liu XJ (2009) Antiapoptotic role for ornithine decarboxylase during oocyte maturation. *Mol. Cell. Biol.* **29**, 1786–1795.

## Supporting Information

Additional Supporting Information may be found in the online version of this article at the publisher's web-site.

**Fig. S1** Typical images of euploid (a), hypoploid (b) and hyperploid (c and d) oocytes.

**Fig. S2** DFMO drinking water schedules.

**Fig. S3** Metaphase I spindle morphology.

**Table S1** Detailed breakdown of data listed in Table 1 (DFMO in vitro).

**Table S2** Detailed breakdown of data listed in Table 3 (DFMO in vivo).

**Table S3** Detailed breakdown of data listed in Table 4 (2-cell embryo karyotypes).

**Table S4** Detailed breakdown of data listed in Table 5 (DFMO in F1 mice).

**Table S5** Detailed breakdown of data shown in Table 6 (heterozygous odc mice).

**Table S6** Detailed breakdown of data listed in Table 7 (putrescine in older mice).